PNAS RESEARCH ARTICLE | PHYSIOLOGY

Steroidogenic factor 1 (SF-1; *Nr5a1*) regulates the formation of the ovarian reserve

Camilla H. K. Hughes[a], Olivia E. Smith[a], Marie-Charlotte Meinsohn[b,c], Mylène Brunelle[d], Nicolas Gévry[d], and Bruce D. Murphy[a,1]

Edited by Laurinda Jaffe, UConn Health, Farmington, CT; received December 13, 2022; accepted June 12, 2023

The ovarian follicle reserve, formed pre- or perinatally, comprises all oocytes for lifetime reproduction. Depletion of this reserve results in infertility. Steroidogenic factor 1 (SF-1; *Nr5a1*) and liver receptor homolog 1 (LRH-1; *Nr5a2*) are two orphan nuclear receptors that regulate adult endocrine function, but their role in follicle formation is unknown. We developed models of conditional depletion of SF-1 or LRH-1 from prenatal ovaries. Depletion of SF-1, but not LRH-1, resulted in dramatically smaller ovaries and fewer primordial follicles. This was mediated by increased oocyte death, resulting from increased ovarian inflammation and increased Notch signaling. Major dysregulated genes were Iroquois homeobox 3 and 5 and their downstream targets involved in the establishment of the ovarian laminin matrix and oocyte-granulosa cell gap junctions. Disruptions of these pathways resulted in follicles with impaired basement membrane formation and compromised oocyte–granulosa communication networks, believed to render them more prone to atresia. This study identifies SF-1 as a key regulator of the formation of the ovarian reserve.

ovarian reserve | primordial follicle | orphan nuclear receptor | steroidogenic factor 1 | follicle assembly

Significance

In this study, we identified the orphan nuclear receptor Steroidogenic factor 1 (SF-1) as a regulator of the formation of the ovarian follicle reserve, which is composed of all the primordial oocytes and the somatic cells that surround and support them. Depletion of SF-1 resulted in dramatically reduced ovarian reserve due to impaired follicular formation and increased oocyte death. This was caused by dysregulated deposition of ovarian laminins, impaired oocyte–granulosa cell communication, and disrupted KIT-KITL and Notch signaling. This study reveals an important mechanism of ovarian reserve establishment, indicating that SF-1 is a key factor in establishing the reserve of follicles that determines lifetime fertility. Therefore, this work provides a foundation for future investigations of premature ovarian insufficiency and menopause.

The frequency of infertility has increased in recent decades, primarily due to couples choosing to delay childbearing (1). It affects some 15% of couples (2), and approximately 40% of these cases are attributable to ovarian dysfunction (3). A major cause of infertility is aging and consequent depletion of the ovarian follicle reserve. This bank of primordial follicles, established prior to or around the time of birth in mammals, comprises the nonrenewing pool of oocytes and supporting cells representing the lifetime fertility potential of the ovary (4). Follicle depletion accompanies the natural aging process and is the primary cause of menopause in humans. An ovarian disorder, premature ovarian insufficiency (POI), manifests as early infertility. This condition is characterized by loss of ovarian function and the onset of menopause prior to the age of 40 (5). This is due to decline in the population of primordial follicles, but the underlying cause of POI is known in only some 50% of cases (6). If the ovarian reserve is amenable to pharmacological modulation, it becomes an attractive target for the development of therapeutic interventions to address conditions where follicle depletion is the cause of infertility.

The formation of the population of primordial follicles, known as follicle assembly, occurs pre- or perinatally in mammals and has been most studied in mouse models. Prior to the initiation of this assembly, oocytes are aggregated into nests, also referred to as cysts (4). In the complex process that ensues, oocyte nests break down as somatic cells invade into them (4). Oocytes not surrounded by a layer of somatic cells suffer apoptotic demise. In the mouse, follicle assembly is initiated on approximately embryonic day (ED)17.5 and completed around postnatal day (PND) 4 (7, 8). Following formation of the pool, the progressive and irreversible activation of primordial follicles begins (7). Not all the activated follicles will complete growth, as the majority will undergo atresia, mostly prior to pubertal onset.

The orphan nuclear receptors steroidogenic factor 1 (SF-1; *Nr5a1*) and liver receptor homolog 1 (LRH-1; *Nr5a2*) have well-established roles in the function of the adult ovary (9, 10). Consequences of mutations in the gene encoding SF-1 include POI (11–13), suggesting that this receptor plays a key role in the regulation of the ovarian reserve. Information on the consequences of LRH-1 mutation in humans is scarce, but much has been learned from murine models. LRH-1 is expressed abundantly and specifically in granulosa cells of a subset of primordial follicles (14) and all primary, preantral, and antral follicles (9). Conditional depletion of LRH-1 from the germ cell nest stage or from the antral follicle stage forward results in anovulation and infertility (15, 16). Depletion of LRH-1 from the germ cell nest stage forward also results in an inhibition of follicular activation, which is manifest as an increased population of primordial follicles and a reduced number of primary follicles (14). In contrast, SF-1 is expressed in the urogenital ridge from at least ED9, prior to the differentiation of the gonadal primordium from the

Author contributions: C.H.K.H., O.E.S., N.G., and B.D.M. designed research; C.H.K.H., O.E.S., M.-C.M., and M.B. performed research; C.H.K.H., M.B., N.G., and B.D.M. analyzed data; and C.H.K.H., O.E.S., M.-C.M., M.B., N.G., and B.D.M. wrote the paper.

The authors declare no competing interest.

This article is a PNAS Direct Submission.

[1]To whom correspondence may be addressed. Email: bruce.d.murphy@umontreal.ca.

This article contains supporting information online at https://www.pnas.org/lookup/suppl/doi:10.1073/pnas.2220849120/-/DCSupplemental.

Published July 26, 2023.

developing adrenal gland. This primordium forms on ED10, and the resulting progenitor cell population is dependent on SF-1 and the WT1 transcription factor (WT1) for survival and expansion (17). Thus, germline loss of SF-1 results in gonadal agenesis (18). The gonadal expression of SF-1 is maintained until ED12.5, after the divergence of the ovarian and testis fates (19). Thereafter, SF-1 expression is maintained or slightly reduced in the ovary, while it is comparatively greater in the testis (19, 20).

Ovarian depletion of SF-1 results in infertility, the occurrence of which depends on the developmental stage of the ovary at which depletion is initiated. Ovary-specific conditional knockout from the germ cell nest stage forward, using Cre recombinase driven by the anti-Müllerian hormone type two receptor (*Amhr2*) promoter (21), was without effect on ED14.5 or ED16.5 (22). In contrast, at 21 d of age, these mice had fewer follicles at every stage of development, compared to wild-type counterparts (23). The females were completely infertile, a condition attributed to impaired responsiveness of the ovary to gonadotropin stimulation (23). In contrast, depletion of SF-1 from the antral follicle forward [cytochrome P450, family 19, subfamily a, polypeptide 1(*Cyp19a1*)-Cre] had no effect, while depletion from the developing corpus luteum [progesterone receptor (*Pgr*)-Cre] resulted in subfertility (24, 25). Together, these findings indicate a role for SF-1 in early ovarian development, including follicle assembly and growth.

Given the evidence implicating LRH-1 and SF-1 in regulation of follicle populations, our objective was to determine the mechanisms by which these factors dictate establishment of the ovarian reserve, including in oocyte cyst breakdown and follicular assembly. To this end, we established a model of LRH-1 or SF-1 conditional depletion from the stage of formation of the germ cell cyst forward. While depletion of LRH-1 had no apparent effect, there was a dramatically reduced ovarian reserve in SF-1 cKO mice. Several key follicular mechanisms were disrupted in SF-1 cKO ovaries, including the Notch signaling pathway, the kit ligand (KITL) pathway, and pathways associated with establishment of the follicular basement membrane and oocyte–granulosa cell communication. Together, these disruptions led to increased oocyte death and a greatly diminished ovarian reserve, indicating that SF-1 has major mechanistic significance for lifetime fertility in mammals.

Results

The Ovarian Expression of SF-1 and LRH-1. Oocyte cyst breakdown begins as early as ED17.5 in the mouse, and few early follicles are observed around this time (7, 8). Primordial follicle assembly continues through PND1 and is mostly complete by PND4 (Fig. 1*A*) (7, 8). To validate the use of the *Amhr2*-Cre-mediated depletion model as a tool to investigate the role of LRH-1 and SF-1 in the processes of oocyte cyst breakdown and primordial follicle assembly, we undertook temporal analysis of AMHR2 expression. The *Amhr2* transcript was detectable in the wild-type fetal ovary on ED17.5, PND1, and PND4 by qPCR (Fig. 1*B*) and on ED17.5 by in situ hybridization (RNAscope) (Fig. 1*C*). AMHR2 protein was detectable by immunohistochemistry at the same developmental times (Fig. 1*D*). Next, we evaluated the temporal expression of SF-1 and LRH-1 in the wild-type murine ovary during the period of primordial follicle assembly. There was a substantial increase in *Nr5a2* on PND4 compared to ED17.5 and PND1 (Fig. 1*E*). LRH-1 was not expressed on ED17.5 but was detectable in the pregranulosa cells of a subset of primordial follicles on PND1 (Fig. 1*F*), consistent with our previous observation of LRH-1 on PND4 (14). In contrast, SF-1 was strongly and specifically expressed in all somatic cells as early as ED17.5, but not oogonia or oocytes, and its abundance did not change appreciably throughout primordial follicle assembly (Fig. 1 *G* and *H*).

To explore the evolutionary conservation of SF-1 and LRH-1 expression during the developmental trajectory of the ovary, we evaluated the expression in silico of *Nr5a1* and *Nr5a2* transcripts in diverse species, including humans, marsupials, and birds, using the Evo-Devo database [https://apps.kaessmannlab.org/evodevoapp/; (26). In all six species analyzed, *Mus musculus* (mouse), *Rattus norvegicus* (rat), *Homo sapiens* (human), *Oryctolagus cuniculus* (rabbit), *Monodelphis domestica* (opossum), and *Gallus gallus* (chicken), *Nr5a1* was robustly expressed before and throughout the period of follicular assembly, whereas *Nr5a2* expression was nearly undetectable (Fig. 2), confirming our previous observation. The prenatal detection of SF-1 in this wide range of species led us to infer that there is a role for this factor in development of the primordial follicle population that is conserved across vertebrate taxae.

Next, we confirmed the effectiveness of the *Amhr2*-Cre in depletion of ovarian SF-1 and LRH-1. On ED17.5 (*SI Appendix*, Fig. S1 *A* and *B*), PND1 (*SI Appendix*, Fig. S1 *C* and *D*), and PND4 (*SI Appendix*, Fig. S1 *E* and *F*), both *Nr5a1* transcripts and SF-1 protein were substantially depleted as a result of Cre-mediated recombination. Similar patterns of depletion were observed in LRH-1 cKO mice on PND1 (*SI Appendix*, Fig. S2 *A* and *B*). To confirm that *Amhr2*-Cre-mediated excision was restricted to the ovary, other sites of SF-1 expression, the adrenal gland and spleen, were evaluated. On ED17.5 and PND1, the relative abundance of *Nr5a1* was unaffected by genotype in these tissues (*SI Appendix*, Fig. S1 *G*, *H*, *J*, and *K*). In addition, the abundance of *Cyp11a1*, a steroidogenic enzyme and key downstream target of SF-1 (38), was unchanged in SF-1 cKO adrenals (*SI Appendix*, Fig. S1 *I* and *L*) indicating ovarian specificity of *Amhr2*-Cre depletion. The hypothalamus and pituitary are also sites of SF-1 expression. Nevertheless, previous work has demonstrated normal follicular development to the secondary or early antral stage in mice with hypothalamus- (39) or pituitary gonadotrope-specific (40) depletion of SF-1. Therefore, evaluation of the hypothalamus and pituitary even for nonspecific Cre activity or SF-1 depletion was judged irrelevant to evaluation of an ovary-specific phenotype at this early stage of ovarian development. We then used this model to deplete SF-1 and LRH-1 during ovarian development in the mouse, omitting investigations of ED17.5 in the LRH-1 model, given that the LRH-1 signal is undetectable in the ovary at this time.

Phenotypic Effect of Ovarian Depletion of SF-1 and LRH-1. Ovarian volume was not reduced in SF-1 cKO mice on ED15.5 (prior to the beginning of assembly; Fig. 3*A*), despite expression of SF-1 on this day (*SI Appendix*, Fig. S3). ED15.5 ovaries were also histologically indistinguishable from control counterparts collected on the same day (Fig. 3*B*). In distinct contrast, on ED17.5, PND1, and PND4, loss of SF-1 substantially reduced ovarian volume and prevented the ovarian growth observed in control ovaries (Fig. 3*A* and *SI Appendix*, Fig. S4). In addition, the number of oocytes in nests tended to be reduced in cKO ovaries on ED17.5 and PND1 (Fig. 3 *C* and *D*). Thus, the onset of a phenotype resulting from depletion of SF-1 with *Amhr2*-Cre is approximately concurrent with the onset of oocyte nest breakdown and follicular assembly.

In keeping with the ovarian volume results, the number of primordial follicles was substantially reduced in cKO ovaries during the period of primordial follicle assembly (PND1; Fig. 3*E*). To test whether the reduced primordial follicle population was a result of a reduced oocyte population, we calculated the number

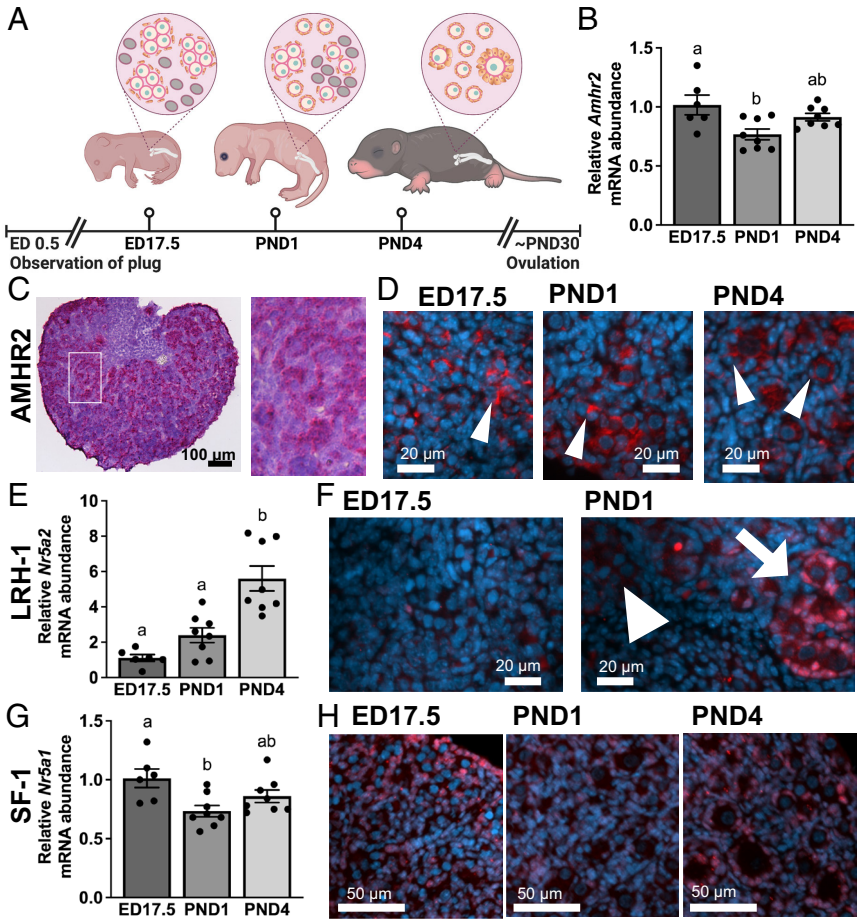

Fig. 1. LRH-1, SF-1, and AMHR2 in wild-type ovaries on ED17.5, PND1, and PND4. (*A*) Schematic diagram showing the time points evaluated and the accompanying events in the ovary (created using biorender.com). (*B*) Gene expression of *Amhr2* in ovaries from ED17.5, PND1, and PND4 as assessed by qPCR. (*C*) RNAscope in situ hybridization for *Amhr2* in ED17.5 ovaries, including lower and higher magnification. (*D*) AMHR2 protein expression in ovaries from ED17.5, PND1, and PND4 as assessed by immunohistochemistry; AMHR2 staining is indicated by narrow triangles. (*E*) Gene expression of *Nr5a2* in ovaries from ED17.5, PND1, and PND4. (*F*) Immunostaining for LRH-1 protein in ED17.5 and PND1 ovaries. The arrow indicates LRH-1 positive primordial follicles, while the triangle indicates an LRH-1 negative germ cell nest. (*G*) Gene expression of *Nr5a1* in ovaries from ED17.5, PND1, and PND4. (*H*) Immunostaining for SF-1 protein in ED17.5, PND1, and PND4 ovaries. For the qPCR experiment, n = 6 to 8, as shown on graphs; n = 3 for immunohistochemistry and representative images are shown. In all immunofluorescence images, the protein of interest is shown in red, and nuclei are counterstained with DAPI. Data were analyzed by ANOVA followed by individual comparison of means using the Tukey post hoc test. Bar graphs represent the mean ± SEM, and bars with common superscript letters were not different at $P < 0.05$.

of primordial follicles per oocyte. This population was also reduced in cKO ovaries (Fig. 3*E*), demonstrating that there was a reduced rate of primordial follicle assembly. The phenotype of reduced ovarian reserve was maintained on PND4 (Fig. 3*F*) and PND13 (Fig. 3*G*), showing that conditional depletion of SF-1 has a persistent effect on the size of the ovarian reserve.

Quantification of primordial follicles in LRH-1 cKO mice on PND1 revealed no difference in either follicle or oocyte numbers (*SI Appendix*, Fig. S5). In addition, there was no phenotype of reduced ovarian volume (*SI Appendix*, Figs. S4 and S5). Despite the lack of a histological phenotype, qPCR analysis of regulators of cyst breakdown and primordial follicle assembly in LRH-1 cKO mice revealed changes in transcript abundance of anti-Müllerian hormone (*Amh*) on PND1, while thirteen other genes were unaffected and three [growth differentiation factor 9 (*Gdf9*), cadherin 1 (*Cdh1*), and snail family zinc finger 1 (*Snai1*)] tended to change ($P = 0.08$). In summary, the change in transcript abundance in response to loss of LRH-1 was minor to undetectable (*SI Appendix*, Fig. S5), consistent with a lack of histological phenotype.

To further confirm the lack of role of LRH-1 in primordial follicle assembly, we generated a line of mice with depletion of both LRH-1 and SF-1 (double cKO). These mice recapitulated the phenotype of SF-1 cKO mice on PND4, with a substantially reduced pool of ovarian primordial follicles and reduced ovarian size (Fig. 3*H*). Nevertheless, double cKO follicular populations did not differ from those in the SF-1 cKO model, indicating no additive effect. In summary, depletion of SF-1, but not LRH-1, repressed oocyte nest breakdown and follicular assembly, thus substantially reducing the ovarian reserve.

Depletion of SF-1 Results in Impaired Follicular Formation: Physiological Mechanisms. To delineate the SF-1-regulated mechanisms altering follicle assembly, we compared transcriptional profiles of ovaries collected from SF-1 cKO and control mice on ED17.5, PND1, and PND4 (Datasets S1–S7, NCBI Gene Expression Omnibus, accession number GSE216420). Analysis of the mRNAseq dataset revealed that age and genotype were the primary drivers of variation, as exemplified by principal component analysis (Fig. 4*A*). On both PND1 and PND4, more genes were up-regulated than down-regulated by the loss of SF-1 (Fig. 4*B*). Thirty-six mRNAs with known importance in ovarian development were evaluated by qPCR, and there was clear agreement of qPCR with mRNAseq results (*SI Appendix*, Tables S1 and S2). There was a substantial (~20 to 50%) overlap among transcripts that differed in SF-1 cKO ovaries on each of the three days investigated, suggesting that the disrupted transcriptional program caused by SF-1 depletion is maintained through ovarian development (Fig. 4*C*). To identify the salient disruptions resulting from loss of SF-1, pathway analysis was conducted on transcripts that differed in SF-1 cKO ovaries on all three days of ovarian development, comprising 216 genes in total (Fig. 4*C*). Among the pathways we identified were embryonic organ morphogenesis and gonad development (Fig. 4*D* and Dataset S8), pathways that included the Iroquois homeobox (IRX) transcription factors *Irx3* and *Irx5*.

Gene ontology analysis of transcripts up-regulated in response to SF-1 depletion on ED17.5 revealed increases in transcripts associated with extracellular matrix formation and cell migration. Down-regulated pathways included hormone production and cell signaling (*SI Appendix*, Fig. S6). Notably, gonad development was

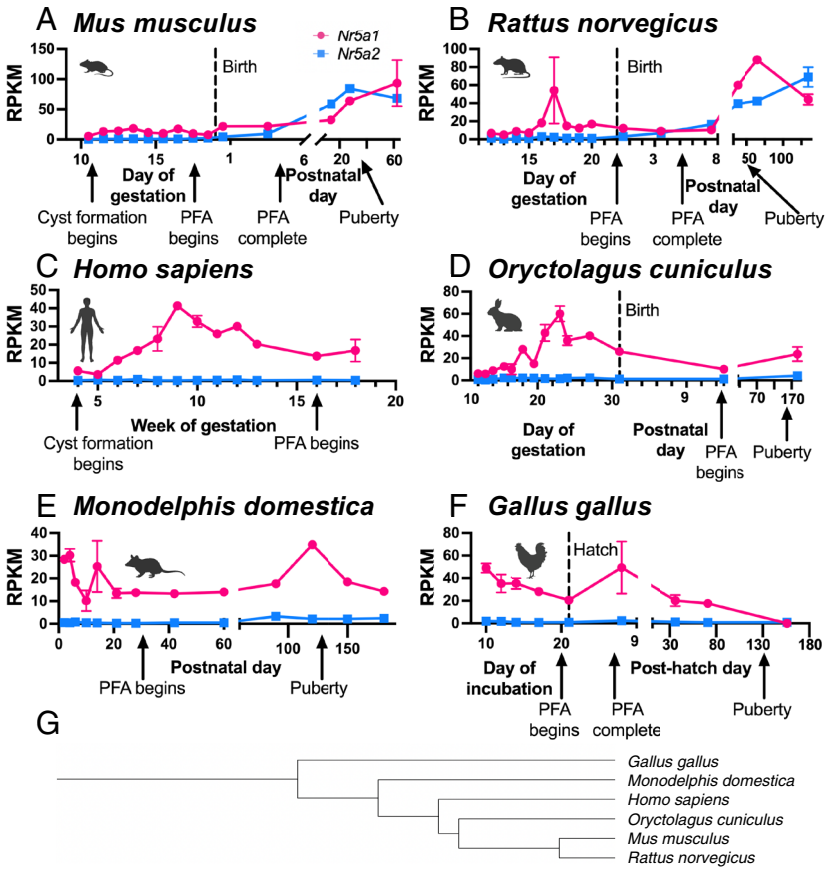

Fig. 2. Evolutionary conservation of *Nr5a1* and *Nr5a2* expression before, during, and after primordial follicle assembly (PFA). *Nr5a1* (pink) and *Nr5a2* (blue) abundance in (*A*) *Mus musculus* (mouse); (*B*) *Rattus norvegicus* (rat); (*C*) *Homo sapiens* (human); (*D*) *Oryctolagus cuniculus* (rabbit); (*E*) *Monodelphis domestica* (opossum); and (*F*) *Gallus gallus* (chicken). Timing of ovarian developmental events labeled on graphs is approximate and based on literature reports (27–36). Points represent the mean, with error bars showing ± SEM. (*G*) Evolutionary tree showing relationships among the six species evaluated, generated using the Interactive Tree Of Life online tool (37).

among the down-regulated pathways, highlighting the importance of SF-1 in ovarian development. Conditional depletion of SF-1 on PND1 resulted in increases in transcripts in pathways associated with extracellular matrix and cell migration and downregulation of pathways related to metabolism.

More than 84% of the transcripts that differed in SF-1 cKO ovaries relative to control had a predicted *Nr5a1*/*Nr5a2* motif found in the territory of the gene, including proximal sites 5.0 kb upstream and 1.0 kb downstream and distal sites up to 500 kb. This compares to identification of predicted *Nr5a1*/*Nr5a2* motifs in only 30% of genes that did not change in SF-1 cKO ovaries (Fig. 4*E* and Dataset S9). In addition, transcripts that changed in SF-1 cKO ovaries had more total *Nr5a1*/*Nr5a2* motifs in cis-regulatory regions of corresponding genes than did unaffected genes (*SI Appendix*, Fig. S7). This illustrates that the observed changes are likely directly regulated by SF-1.

It is known that IRX3 and IRX5 are essential for formation of granulosa cell basement membranes in follicular assembly (41, 42). The transcripts encoding these homeobox factors were down-regulated in SF-1 cKO ovaries (Fig. 5*A*), and the cis-regulatory regions of the genes had the predicted *Nr5a1*/*Nr5a2* motifs (Dataset S9). Their inhibition in the cKO model was confirmed by in situ hybridization (Fig. 5*B*). The granulosa cell basement membrane is composed primarily of laminins, and its formation is regulated by IRX3 and IRX5 (42). Thus, the potential exists for IRX genes to be mechanistic regulators downstream of SF-1 action in the perinatal ovary. Indeed, in the SF-1 cKO ovary, there is a switch in the aggregate laminin composition, with laminin alpha (*Lama*)1 and *Lama3* decreasing and *Lama2*, *Lama4*, and *Lama5* increasing (Fig. 5*C*). Reduced *Lama1* by qPCR confirmed the observed depletion of this transcript (Fig. 5*D*). The changes in laminin composition in the cKO ovary resulted in an overall increase in total ovarian laminin protein (Fig. 5 *E* and *F*) and completely disrupted ovarian laminin deposition (Fig. 5*F*). In control ovaries, a single, distinct follicular laminin basement membrane was evident, while in cKO ovaries, laminin was distributed throughout the ovarian stroma and between granulosa cells, in contrast to the normal pattern of organization (Fig. 5*F* and *SI Appendix*, Fig. S8). IRX3 and IRX5 also regulate formation of oocyte-granulosa cell gap junctions (42). In this context, the deposition of connexin 43 (CX43) protein was disrupted in SF-1 cKO ovaries, similar to that observed in IRX3 and IRX5 mutants (42) (*SI Appendix*, Fig. S9). Changes to laminins and gap junctions would be expected to result in misassembled follicles. Indeed, in ovaries collected from mature SF-1 cKO mice, inappropriately formed, disorganized follicles with small oocytes were evident (Fig. 5*G*). Taken together, these results demonstrate an essential role for SF-1 in the formation of the follicular structure and the granulosa–oocyte communication network.

Depletion of SF-1 Results in Increased Frequency of Oocyte Death. To determine whether loss of SF-1 alters any normal follicular assembly processes, the global RNA analysis of temporally regulated (PND1 vs. ED17.5) transcripts in control mice (*SI Appendix*, Fig. S10) was compared to that from the cKO ovary. In total, there were 317 transcripts that changed between ED17.5 and PND1 (Padj < 0.05; log2 fold change > |1|) in control ovaries and failed to change in the cKO tissue (Padj > 0.15; log2 fold change < |1|; Fig. 6*A*). The transcripts for physiological mechanisms that decreased over time only in the control ovaries were immune related, including pathways related to response to pathogens, cell adhesion and chemotaxis, immunodeficiency, and

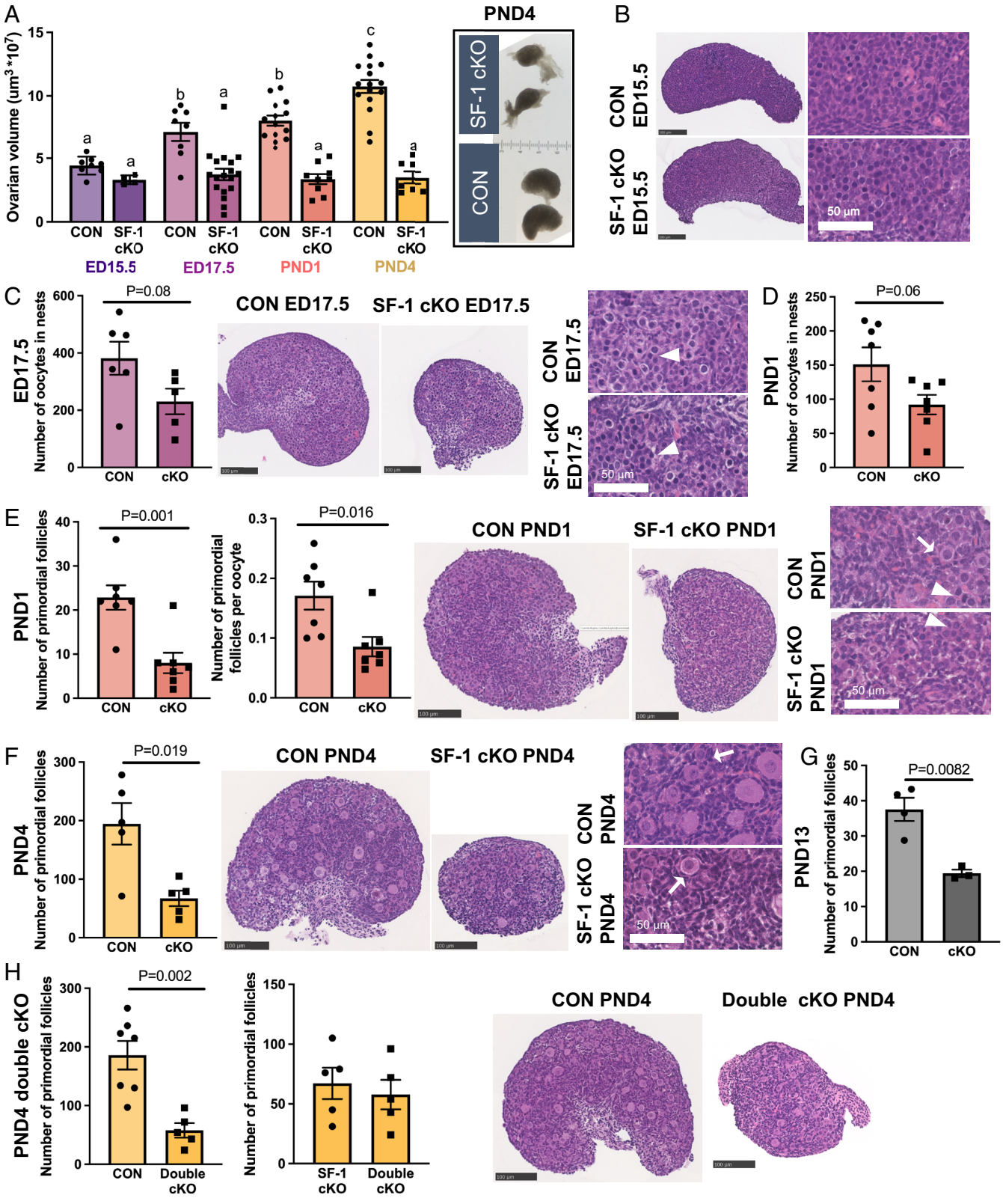

Fig. 3. Phenotypic characterization of perinatal SF-1 cKO ovaries. (*A*) Effect of depletion of SF-1 on ovarian volume. (*B*) Representative histological images of hematoxylin and eosin (H & E)-stained SF-1 CON and cKO ovaries on ED15.5. (*C*) Representative histological images of hematoxylin and eosin (H & E)-stained SF-1 CON and cKO ovaries on ED17.5 and effect SF-1 depletion on oocytes remaining in cysts on ED17.5. (*D*) Effect SF-1 depletion on oocytes remaining in cysts on PND1. Effect of SF-1 depletion on primordial follicle populations on PND1 (*E*), PND4 (*F*), and PND13 (*G*) and representative histological images of hematoxylin and eosin (H & E)-stained SF-1 CON and cKO ovaries for PND1 (*E*) and PND4 (*F*). (*H*) Quantification of follicle populations on PND4 following depletion of both SF-1 and LRH-1 (double cKO), comparison to SF-1 single cKO, and representative histological images from the same day. For oocyte and follicle counts, sections were taken at regular intervals through the whole ovary, and thus, counts are a representative subsample of all follicles in an ovary. The number of replicates is as shown on graphs; n = 3 to 7 for oocyte and follicle count experiments and n = 4 to 18 for ovarian volume. In each ovarian cross-section image, the dark gray (Scale bar represents 100 µm.) Bar graphs represent the means, with error bars showing ± SEM. Data were analyzed by the *t* test.

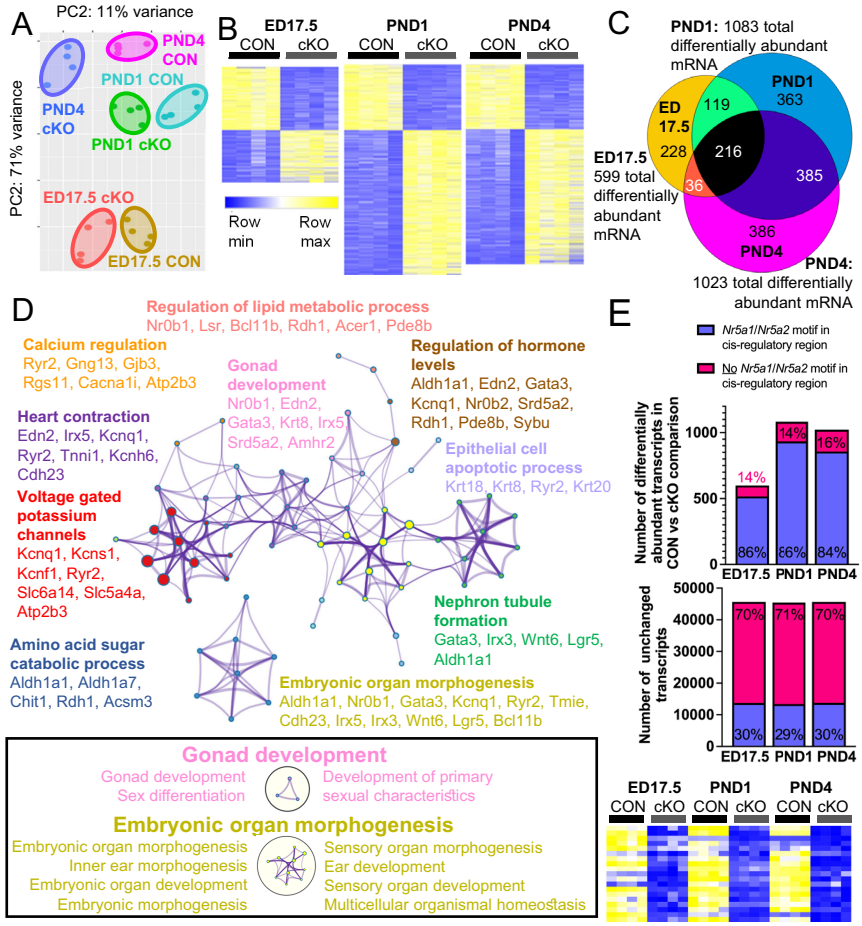

Fig. 4. mRNAseq of SF-1 cKO and control ovaries demonstrates changes to gonadal and organ development pathways. (*A*) Principal component analysis showing clustering of the six groups. (*B*) Heatmaps showing differentially abundant mRNA (padj < 0.05; log2 fold change > |1| within each individual pairwise comparison, performed in DEseq2) in the SF-1 cKO vs. control comparison on ED17.5, PND1, and PND4. (*C*) A Venn diagram depicting the commonalities among datasets in the number of genes affected by the depletion of SF-1 on each of the three days of ovarian development. The number of regulated genes in each comparison is shown outside of the diagram, while the number of common genes for each comparison is shown in each overlapping segment. (*D*) Pathway analysis of the genes down-regulated by depletion of SF-1 on ED17.5, PND1, and PND4, with selected genes from each pathway shown on the network diagram. Reclustering (boxed) and a heatmap (genes: *Aldh 1a1, Amhr2, Bcl11b, Cdh23, Edn2, Gata3, Gpr55, Irx3, Irx5, K cnq1, , Krt8, Lgals2, Lgr5, Lsr, Nr0b1, Ryr2, Srd5a2, Tmie*, and *Wnt6*) depict pathways of interest, gonad development, and embryonic organ morphogenesis. (*E*) Proportion of transcripts that changed (Padj < 0.05; log2 fold change > |1|) in SF-1 cKO ovaries that also have the *Nr5a1/Nr5a2* motif in the cis-regulatory region, as compared to the proportion of transcripts that did not change ($P > 0.05$; log2 fold change < |1|) with the motif. N = 4 per group for mRNAseq. In both heatmaps, yellow indicates the maximum value within a row, while blue indicates the minimum value.

phagocytosis (Fig. 6 *A* and *B* and *SI Appendix*, Fig. S11). These results suggest the presence of an inappropriate inflammatory environment in SF-1 cKO ovaries, which may be either a cause or consequence of increased oocyte death.

We hypothesized that in addition to resulting in inappropriately formed follicles, depletion of SF-1 would result in oocyte death during oocyte cyst breakdown. One potential cause is inappropriate inflammation in cKO ovaries, as described above. Notch signaling, a highly conserved mechanism of intercellular communication, is also known to promote oocyte demise during follicular assembly. Indeed, inhibition of the Notch pathway via granulosa-specific depletion of Notch receptor (NOTCH) two results in increased oocyte survival (43). We found that elements of the Notch pathway were up-regulated in cKO ovaries (Fig. 6*C*), including Notch receptors (*Notch1*, *Notch2*, *Notch3*, and *Notch4*), Notch ligands [Delta-like canonical notch ligand (*Dll*)1, *Dll4*, and Jagged canonical notch ligand 1(*Jag1*)], and Notch regulators [LFNG O-fucosylpeptide 3-beta-N-acetylglucosaminyltransferase (*Lnfg*) and MFNG O-fucosylpeptide 3-beta-N-acetylglucosaminyltransferase (*Mfng*)]. These changes were confirmed by qPCR (*SI Appendix*, Fig. S12 and Tables S1 and S2). We next evaluated well-known markers of apoptosis in cKO and CON ovaries and found that these were mostly unchanged (*SI Appendix*, Fig. S13 *A* and *B*). A key mechanism of oocyte elimination is the DNA damage response pathway (44, 45). All genes associated with the gene ontology (GO) term DNA damage response were assessed, and a subset was found to be affected in SF-1 cKO, particularly on ED17.5 (*SI Appendix*, Fig. S14), suggesting modulation of the DNA damage response may be an early mechanism of SF-1-mediated increase in oocyte death. The complement pathway has been implicated as an effector in oocyte attrition downstream of the DNA damage mechanism (46). Remarkably, among 61 genes associated with the GO term activation of complement, 15 increased in cKO ovaries on PND1, a day of maximal oocyte attrition (Fig. 6*D*), and eight increased in cKO ovaries on ED17.5 (*SI Appendix*, Fig. S15). These findings implicate the immune-mediated complement pathway as a factor in the increased oocyte attrition observed in SF-1 cKO ovaries.

Glycogen synthesis kinase-3 beta (*Gsk3b*) is upstream of the oocyte attrition process mediated through DNA damage checkpoint mechanisms (47) and modulates apoptosis via effects on the translocation of beta-catenin and *Trp63* expression (47). Although the specific mechanism involving *Gsk3b* seems to be largely unaffected by depletion of SF-1 (*SI Appendix*, Fig. S16*A*), canonical Wnt signaling was modestly modulated by depletion of SF-1, particularly on PND1 (*SI Appendix*, Fig. S16*B*).

Autophagy has also been implicated in oocyte survival and death during primordial follicle assembly, with both excess autophagy (48) and reduced autophagy (49) causing oocyte death. Many genes associated with the GO term regulation of autophagy changed in SF-1 cKO ovaries, with the most distinct changes occurring on PND1 (*SI Appendix*, Fig. S17 *A* and *B*). One outcome of autophagy is an increase in lysosome formation and lysosomal degradation. In cKO ovaries on PND1, transcripts coding for cathepsins, effectors of this pathway, were in substantially greater abundance relative to control counterparts (*SI Appendix*, Fig. S17*C*). This increase in lysosomal degradation is a potential driver of increased oocyte death in SF-1 cKO ovaries.

To confirm the increase in oocyte death in SF-1 cKO ovaries, a TUNEL assay was performed to label dead oocytes. On ED17.5 and PND1, when oocyte attrition is rampant, dead oocytes were

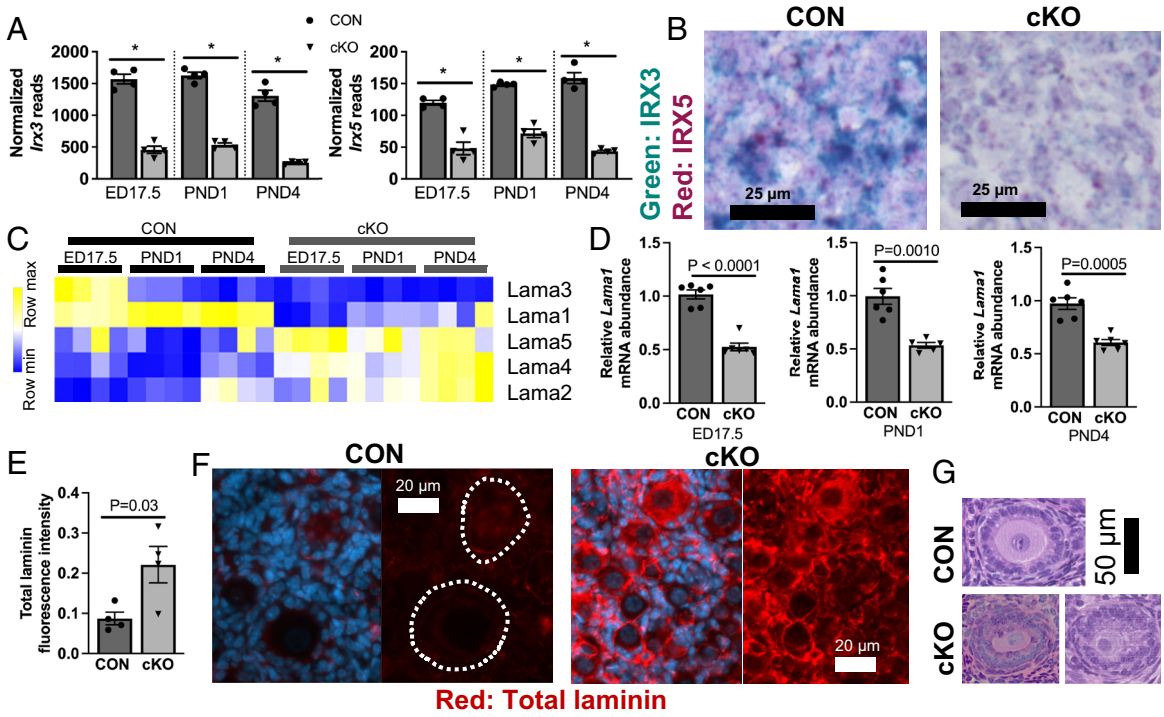

Fig. 5. Conditional depletion of SF-1 results in downregulation of *Irx3* and *Irx5* and dysregulation of ovarian laminin. Abundance of *Irx3* and *Irx5* transcript from mRNAseq (*A*) and in situ hybridization (*B*) and of laminin transcripts by mRNAseq (*C*), qPCR (*D*) and total laminin protein on PND4 by immunofluorescence (*E* and *F*). The dashed white lines in F indicate a normal laminin basement membrane around primary follicles in the control ovaries. In immunofluorescence images, the protein of interest is red, and nuclei are blue (DAPI). The red channel only (laminin) image is also shown. (*G*) H&E images of follicles from an adult control and SF-1 cKO mice. N = 4 to 6, as shown on graphs. Data in *A* are mRNAseq data analyzed in DEseq2, and * indicates Padj < 0.05 within the individual pairwise cKO vs. CON comparison shown. Pairwise comparisons of other groups are not shown but are available in Datasets S1–S7. Data in (*D*) and (*E*) were analyzed by the *t* test. In all bar graphs, the bars represent the means, with error bars showing ± SEM.

identified in both SF-1 cKO and CON ovaries, with more oocyte death evident in the cKO ovaries than in control counterparts (Fig. 6*E*). Few dead oocytes were detectable on PND4 in either control or cKO ovaries (*SI Appendix*, Fig. S13*C*). In summary, SF-1 may promote, or perhaps simply permit, the survival of oocytes, as demonstrated by increased oocyte death in SF-1 cKO ovaries.

Depletion of SF-1 Results in Inhibition of the KITL Signaling Pathway. Intercellular signaling regulated by KITL and its interaction with KIT proto-oncogene receptor, tyrosine kinase (KIT), promote cell survival and are among the best-known regulators of follicular activation. This pathway has also been identified as a regulator of germ cell cyst breakdown and follicular assembly (50). Herein, we show that the oocyte-specific receptor *Kit* was unaffected by loss of SF-1 in ED17.5 and PND1 ovaries, but *Kitl* was less abundant on both days (Fig. 7*A*). Ovarian culture experiments tested whether recombinant KITL rescued the phenotype of reduced ovarian reserve. Cultures were initiated at ED17.5, and, after 6 d of treatment, cKO ovaries cultured with KITL had increased ovarian reserve (Fig. 7 *B* and *C*) resulting in a follicular population comparable to untreated control ovaries. Interestingly, in cKO ovaries that were treated with KITL, unusual follicular phenotypes were observed, including double oocyte follicles (Fig. 7*D*) and follicles with large-volume oocytes but flattened, primordial granulosa cells (Fig. 7*E*). This suggests that although KITL treatment partially rescued the phenotype of reduced ovarian reserve, follicular dysfunction remains, perhaps due to the malformation of the laminin follicular basement membrane.

Discussion

SF-1 is an essential regulator of multiple aspects of follicular function. The conservation of its expression throughout the period of follicular assembly in six evolutionarily diverse species, including rodents, marsupials, birds, and humans, implies a role for SF-1 in the establishment of the ovarian reserve. Here, we provide experimental evidence demonstrating a dramatic effect of the depletion of SF-1 on the number of primordial follicles and, consequently, the ovarian reserve in the mouse. This effect is elicited through several interrelated mechanisms, including increases in oocyte death, reduced follicular assembly, and formation of follicles with impaired basement membrane and oocyte–granulosa communication networks. Disrupted signaling pathways resulting in this phenotype included reductions in KITL and IRX signaling and increases in Notch signaling and inflammation (Fig. 8).

We have previously shown that conditional depletion of LRH-1 results in an increase in the population of primordial follicles on PND4 (14), which we initially hypothesized to be the result of an increase in primordial follicle assembly. This proved not to be the case, as, in contrast to the reduced ovarian reserve observed in SF-1 cKO ovaries, there was no discernable morphological phenotype in ovaries of LRH-1 cKO mice on PND1. Further, among 19 transcripts evaluated by qPCR, only *Amh* was affected by depletion of LRH-1 on PND1. Indeed, our results from the LRH-1 cKO, and the lack of additive or synergistic phenotype in the double cKO model, demonstrate that SF-1 is the key regulator of primordial follicle assembly, with no additional role for LRH-1.

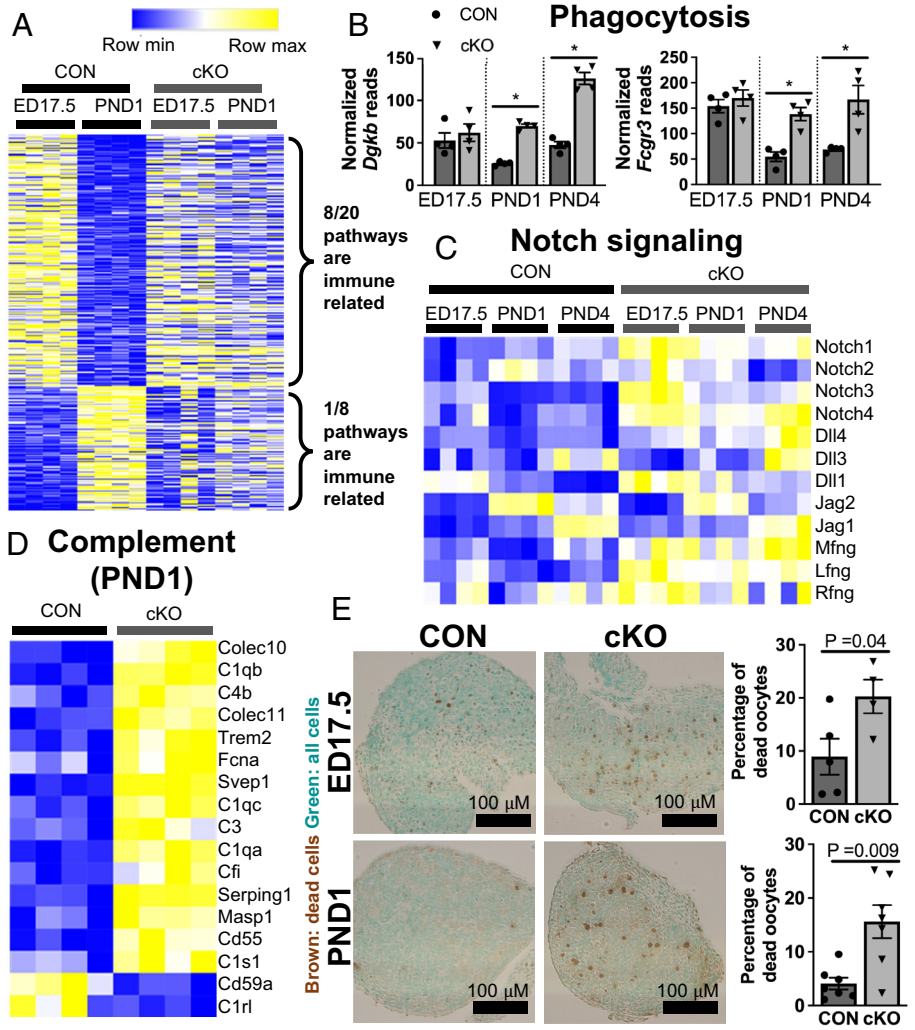

Fig. 6. Conditional depletion of SF-1 results in increased oocyte death, excess ovarian inflammation, and changes to Notch signaling during follicular assembly. (*A*) Heatmap showing the expression of transcripts that changed between ED17.5 and PND1 in control ovaries but failed to change in SF-1 cKO ovaries. Yellow indicates the maximum value within a row, while blue indicates the minimum value. Complete pathway analysis is in *SI Appendix*, Fig. S11. (*B*) Abundance of selected transcripts that regulate phagocytosis, assessed by mRNAseq. Abundance of components of the Notch signaling pathway, regulators of oocyte survival (*C*) and of complement transcripts, and regulators of cellular death downstream of the DNA damage response (*D*), assessed by mRNAseq. (*E*) TUNEL staining and quantification on ED17.5 and PND1, showing dead cells in brown and all cells counterstained in green. As shown on graphs, n = 4 for mRNAseq and n = 4 to 7 for TUNEL assay. Data in (*B*) are mRNAseq data analyzed in DEseq2, and * indicates Padj < 0.05 within the individual pairwise cKO vs. CON comparison. Pairwise comparisons of other groups are not shown but are available in Datasets S1–S7. Data in (*E*) were analyzed by the *t* test. In all bar graphs, the bars represent the means, with error bars showing ± SEM.

Early studies demonstrated that the adrenogonadal primordium does not survive in SF-1 germline knockouts, resulting in adrenal and gonadal agenesis (18). This leads to death of neonates in the first week of life due to inadequate production of adrenal steroids (18). Therefore, ovarian-specific knockout models, including the *Amhr2*-Cre model, have been employed to delineate the essential role of this orphan nuclear receptor in the ovary. In earlier studies, depletion of SF-1 in granulosa cells from ~ED12.5 onward resulted in complete infertility in adult mice, which was attributed to a reduction in all follicular populations, impaired gonadotropin responsiveness, and reduced estradiol production in antral follicles (22, 23). Nevertheless, we have recently shown that SF-1 depletion from granulosa and/or theca cells of antral follicles [cytochrome P450, family 17, subfamily a, polypeptide 1 (*Cyp17a1*)-Cre, *Cyp19a1*-Cre, or both] has no effect on fertility (24). In contrast, depletion from the periovulatory follicle, after the ovulatory signal (*Pgr*-Cre), results in a phenotype of subfertility, accompanied by defects in ovulation, cumulus expansion, and luteinization (25).

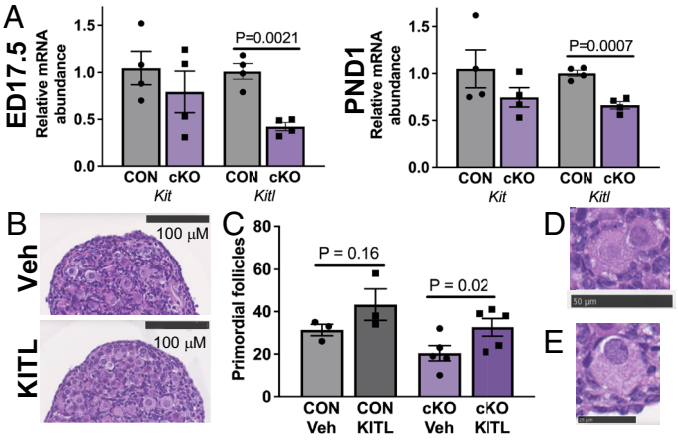

Fig. 7. KITL is downstream of SF-1 and rescues the phenotype of reduced ovarian reserve in SF-1 cKO ovaries. (*A*) Abundance of *Kit* and *Kitl* in ED17.5 and PND1 ovaries, as assessed by qPCR. (*B*) Representative histological images of SF-1 cKO ovaries cultured for 6 d without and with 100 ng/mL KITL. (*C*) Quantification of primordial follicle populations in CON and SF-1 cKO ovaries cultured without and with KITL. (*D*) Multi-oocyte follicles were observed in cKO ovaries cultured with KITL. Error bar = 50 μM. (*E*) Large oocytes with flattened, primordial granulosa cells were observed in cKO ovaries cultured with KITL. Error bar = 25 μM. N = 3 to 5 for both qPCR and ovarian culture experiments as shown on the graphs. The qPCR data were analyzed by the *t* test and ovarian culture data were analyzed by paired *t* test with mouse as pairing factor. In all bar graphs, the bars represent the means, with error bars showing ± SEM.

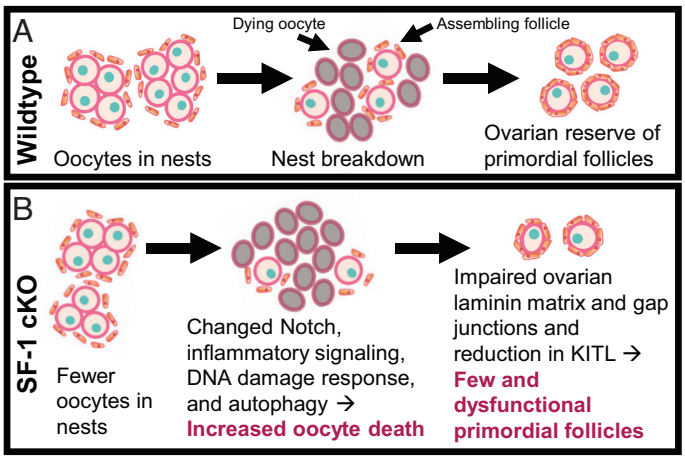

Fig. 8. Summary of the effects of SF-1 depletion on the ovarian reserve. (*A*) Schematic diagram showing events in follicular assembly in wild-type or control ovaries. (*B*) Schematic diagram showing the processes that are disrupted in SF-1 cKO ovaries during follicular development.

Overexpression of SF-1 in the mouse ovary results in polyovular follicles and accumulation of corpora lutea (17, 51). Taken together, these results suggest that the disrupted ovarian phenotype observed in SF-1 cKO mice at later ages is due primarily to the effects of depletion of SF-1 during the process of follicular formation.

Mechanisms of ovarian reserve establishment include the indirect effects and influences of the oocyte. Oogonial mitotic divisions occur from approximately ED11 to ED14.5 in the mouse (52). To this point, we saw no effects of depletion at ED15.5; SF-1 cKO ovaries were of the same size as and histologically indistinguishable from control counterparts. Moreover, although there was modest depletion of SF-1 protein in the cKO model at ED15.5, this depletion did not reach statistical significance. The earliest physiological change observed resulting from depletion of SF-1 was reduction in the number of oocytes in cysts on ED17.5, i.e., before primordial follicle assembly began, consistent with moderately smaller ovaries in cKO mice at this time. The timing of SF-1 depletion relative to oogonial proliferation and oocyte attrition indicates that the discrepancy in the population of oocytes remaining in cysts in SF-1 cKO ovaries is a consequence of increased oocyte death, rather than diminished proliferation. Other studies have identified degenerating oocytes in the ovary before and during the period of assembly (52, 53), and this attrition is an important contributor to determination of the final composition of the ovarian reserve (53). The observed reduction in the number of oocytes in cysts in cKO ovaries on ED17.5 and PND1 and the increase in TUNEL-positive cells on these same days indicates that increased oocyte attrition is a major cause for the reduced ovarian reserve in cKO ovaries and that SF-1 may protect oocytes from death. The reduced expression of SF-1 in the cKO ovary is accompanied by excessive oocyte attrition before and during follicular assembly, resulting in fewer oocytes available to be assembled into follicles.

Another mechanism by which SF-1 may regulate the ovarian reserve is through the Notch signaling pathway since an overexpression of components of this pathway in the cKO ovaries was associated with increased oocyte death. The Notch signaling pathway is a well-known component of the complex that regulates follicular assembly (54). Granulosa-specific depletion of NOTCH2 results in fewer primordial follicles, polyovular follicles, and an increase in the total number of oocytes, mediated partially through reduced oocyte apoptosis (43). Similarly, mice with knockout of LFNG, a Notch regulator, display multiple polyovular follicles (55). Strikingly, ovarian overexpression of SF-1 results in a similar phenotype of polyovular follicles, driven at least partially by dysregulation of Notch signaling (51, 56). These data suggest that inhibition of the Notch pathway results in reduction in oocyte attrition during cyst breakdown, indicating that an increase in Notch in the SF-1 cKO model may be another driver of the increased oocyte attrition.

Despite the clear reduction in the ovarian reserve and increase in dead oocytes in cKO ovaries, changes to apoptosis marker transcript abundance were not remarkable. Although there is evidence that germ cells and oocytes mostly die by apoptosis (54), total loss of germ cells and oocytes far outpaces the observable number of dying cells detectable by cell death assays (53). This fits with our findings that apoptosis markers were mostly unchanged in cKO ovaries and dying cells, while detectable, were relatively few. The DNA damage response system is a well-established mechanism of oocyte elimination (44, 45). Although cKO of SF-1 was without effect on the canonical regulators of the DNA damage response system, *Chek1*, *Chek2*, *Atm*, and *Atr* (45), numerous other regulators of this pathway did change. Of particular note were the dramatic upregulation of *Hic1*, a tumor suppressor (57); *Pmaip1*, a known driver of oocyte apoptosis (58); and *Twist1*, basic helix–loop–helix transcription factor known to promote DNA instability (59). Upstream regulators of the DNA repair pathway include the retrotransposon system, but surprisingly, the transcript produced from the retrotransposon LINE-1 (*L1td1*), which promotes oocyte death (44), was down-regulated in SF-1 cKO ovaries. This suggests that activation of the DNA damage response system in SF-1 cKO ovaries is downstream of this retrotransposon, perhaps induced initially by changes to granulosa cells.

The complement pathway is an immune mechanism of cell elimination that has been implicated downstream of the DNA damage response in oocyte death (46). It was dramatically up-regulated in cKO ovaries, suggesting its importance as a mechanism of oocyte removal in the absence of SF-1. The overall increase in inflammatory pathways in cKO relative to CON ovaries may be either a cause or a consequence of this increased oocyte death. Indeed, our data indicate that there may be an influx into cKO ovaries of macrophages, a cell type associated with elimination of dead cells, as demonstrated by upregulation of a macrophage marker, adhesion G protein-coupled receptor E1 (*Adgre1*). While macrophages have been documented in the fetal mouse ovary (60), a role for immune activation at this stage of ovarian development has yet to be identified.

In addition to mechanisms related to DNA damage response, autophagy is an important mechanism of oocyte removal, with either excess or reduced autophagy leading to loss of the ovarian reserve (48, 49). Although two previously identified ovarian

autophagy regulators [*Sqstm1* and *Kdm1a*; (48) were unchanged in our dataset, a substantial number of other autophagy mediators were dysregulated, particularly on PND1, when oocyte death is rampant. A consequence of activation of the autophagy pathway is induction of lysosomal degradation via proteolytic cathepsins, a mechanism by which oocytes are eliminated (61). Herein, we report that the abundance of several cathepsin transcripts was increased in the cKO ovary, providing another promising marker and mechanism for increased oocyte attrition.

Among other potential regulatory mechanisms are the transcription factors IRX3 and IRX5, which have recently emerged as key regulators of ovarian differentiation and follicular development (41, 42). IRX3 and IRX5 are expressed in the fetal gonad in a sexually dimorphic manner, with expression in the ovary, but not the testis (62). Deletion of the genomic locus encoding both IRX3 and IRX5 results in few follicles forming and none that progress past the primary stage (62). Deletion of both IRX3 and IRX5 from the ovary results in follicles with impaired granulosa cell–oocyte communication and disrupted granulosa cell morphology (42). Among the most distinct changes observed in SF-1 cKO ovaries was a reduction in the expression of both of these transcription factors with the apparent consequence of abnormal and reduced formation of follicles. SF-1 cKO ovaries had disrupted deposition of CX43, in a pattern similar to that seen in the IRX mutant ovaries, suggesting that these follicles may have disrupted granulosa cell–oocyte communication.

A further outcome of IRX deletion in the ovary is defective formation of the laminin basement membrane that provides the structural integrity to the follicle (42, 63). Laminin matrices also regulate cell–cell communication (64), and faulty formation of the basement membrane complex interferes with normal oocyte–granulosa cell interactions. As with the IRX3/IRX5 knockouts, SF-1 cKO ovaries displayed disrupted laminin basement membranes. In contrast to the overall decline in total laminin protein in the IRX3/IRX5 knockouts (42), SF-1 cKO ovaries had excess laminin deposition in the ovarian stroma. Fu et al (42) reported only transcript and protein abundance for total laminin, whereas we observed effects on transcripts encoding several laminin isoforms. Each of these laminin genes had 10 or more predicted *Nr5a1*/*Nr5a2* motifs in the territory of the gene, suggesting direct regulation by SF-1. It may be that expression of some laminins is directly regulated by SF-1, while others are regulated indirectly via IRX3/IRX5, resulting in the discrepancy between our findings and those of Fu et al (42). Although the functional consequences of this laminin excess are not fully understood, these alterations represent clear dysregulation of the follicular growth environment and result in the formation of phenotypically abnormal follicles in adult SF-1 cKO mice.

During normal follicle development, KIT from the oocyte interacts with KITL in the granulosa cells (54). Treatment of cultured wild-type ovaries with KITL promotes cyst breakdown and follicular assembly, and inhibition of the KIT–KITL interaction decreases both processes (50, 65). Our rescue of the ovarian reserve in cKO ovaries with KITL in culture provides evidence that SF-1 drives the expression of KITL to induce follicular assembly. Some of the follicles resulting from KITL treatment in vitro were phenotypically abnormal and were often polyovular. In addition, larger oocytes surrounded by squamous granulosa cells were present, suggesting oocyte growth in response to KITL without concurrent activation of granulosa cells in cKO ovaries. Thus, although partial recovery of the follicle population was observed, KITL alone is inadequate to fully rescue the impaired ovarian phenotype in cKO ovaries in vitro.

Previous work suggested that fine-tuning SF-1 expression during and after ovarian differentiation is required for normal ovarian development, with prenatal overexpression and underexpression resulting in disrupted ovarian function (51, 56, 66). Given that SF-1 germline knockout results in gonadal agenesis, Combes et al (66) generated a model of hypomorphic SF-1 expression prior to gonadal differentiation using *Cited2* –/– mice. These mice had approximately 80% reduction in SF-1 on ED10, which lasted only approximately 2 d. The *Cited2* –/– ovaries exhibited impaired expression of *Wnt4* and *Foxl2*, suggesting that SF-1 expression is required for ovarian differentiation. In contrast, two SF-1 overexpressing lines displayed a phenotype of polyovular follicles (51, 56), suggesting impaired cyst breakdown and reduced oocyte atresia. Nevertheless, neither model recapitulated the human phenotype of XX ovotesticular or testicular development observed in cases of *Nr5a1* mutation in 46, XX humans (11), suggesting that upregulation of SF-1 alone is inadequate to result in sex reversal. Indeed, multiple suppressors of SF-1 overexpression have been identified, including WT-1 (67) and the FOXL2 (68). Both these transcription factors bind directly to the *Nr5a1* promoter region to elicit their repressive effects, promote ovarian differentiation, and prevent the ectopic differentiation of steroidogenic cells (67, 68). These data, together with our findings, suggest that the regulation of SF-1 abundance and activity in the ovary is dosage sensitive.

In terms of potential limitations of our study, we note that SF-1 and LRH-1 function as unliganded monomers and are constitutively active, and cofactors play an important regulatory role (9). These two nuclear receptors share structural similarities and bind to the same consensus motif but have distinct targets. Differential interaction with cofactors may uniquely control which genes are regulated by SF-1 or LRH-1 (9). Questions relating to both cofactors and upstream regulators merit future investigation. Although we have identified multiple physiological mechanisms by which SF-1 regulates the establishment of the ovarian reserve, it is certain that there are others, as yet undiscovered. In addition, the interrelation among the diverse regulatory factors disrupted following SF-1 depletion is not fully understood.

In all studies using a model of conditional depletion, a limitation is failure to completely eradicate the protein of interest. We employed the *Amhr2*-Cre model (21) to deplete SF-1 and LRH-1 specifically from the pregranulosa cells from approximately ED12.5 forward. This Cre model has been used by other groups to investigate the processes of germ cell cyst breakdown and primordial follicle formation (43). Although the expression of both LRH-1 and SF-1 was reduced to a fraction of their normal abundance, detectable transcript and protein remained. Perhaps with deletion, rather than depletion, of the genes of interest, a more profound phenotype would have been observed. In addition, some investigators have reported germline knockout (69) or widespread Cre-mediated recombination in tissues that do not express AMHR2 (70) in this model. Nevertheless, this phenomenon appears rare, as nearly 100 other publications report use of *Amhr2*-Cre models but do not note nonspecific or off-target recombination (71). We assessed two other key sites of SF-1 activity, the spleen (72) and the adrenal (18), and found them to be free from *Amhr2*-Cre-mediated SF-1 depletion. Thus, the *Amhr2*-Cre model was judged appropriate for these studies.

In summary, we have shown that depletion of SF-1 profoundly dysregulates follicle assembly through at least three specific mechanisms: dysregulation of IRX3 and IRX5 and consequent malformation of the granulosa cell basement membrane and ovarian laminin matrix; increased oocyte attrition due to up-regulated inflammatory processes and Notch signaling; and impaired oocyte cyst breakdown and follicle formation due to a paucity of KITL. We have demonstrated an essential function for SF-1 in the formation of the ovarian reserve. As mutations in the *Nr5a1* gene

have been linked to POI and infertility (11–13), this orphan nuclear receptor is a potential target for the development of therapeutics to address age-related infertility.

Materials and Methods

Animals and Colony Maintenance. All mouse experiments were conducted according to the guidelines of the Canadian Council of Animal Care and approved by the Université de Montréal (UdeM) Comité d'éthique de l'utilisation des animaux. The mice used were of the C57BL/6 genetic background, were housed in the laboratory animal facility at the UdeM Faculté de médecine vétérinaire, maintained on a 14 h light, 10 h dark cycle, and provided with pelleted feed and water ad libitum.

The *Nr5a1* floxed mice were obtained from The Jackson Laboratory (Stock No. 007041; B6Ei.129P2-Nr5a1tm2Klp/EiJ; referred to as *Nr5a1* f/f) and have been described previously (24, 25, 73), and the *Nr5a2* floxed mice (referred to as *Nr5a2* f/f) have been described in detail by our research group and others (14–16, 74). These mice were bred to mice with Cre-recombinase expression driven by the *Amhr2* promoter (21). Detailed information on genotyping and sample collection is in *SI Appendix, Methods*.

Ovarian Culture. Ovarian culture was conducted as reported previously (14, 65, 75), with complete description in *SI Appendix, Methods*.

Histology and Follicle Quantification. For follicle quantification, fixed ovaries were sectioned at 4 μm, and every 8th section was saved for counting, as previously described (76, 77). Thus, sections were separated by approximately 28 μm, ensuring that no follicles were counted twice and all regions of the ovary were represented. Further detail is in *SI Appendix, Methods*.

RNA Isolation, mRNAseq, and qPCR. Details of RNA isolation, library construction, and qPCR and RNAseq data analysis may be found in *SI Appendix, Methods*. Sequencing was performed at the RNomics platform at Université de Sherbrooke using Illumina NextSeq, with NextSeq® 500/550 High Output Kit v2 (75 cycles). Approximately 15 million reads per sample were generated. Quality was assessed using FASTQC (78), and data were of high quality. Data were analyzed using the GenPipes RNAseq pipeline (Python version 3.9.1 and GenPipes version 4.3.0), with default settings (79) and genome version GRCm38 (mm10). The raw count matrix obtained from GenPipes was normalized and statistically analyzed using DEseq2 (80). mRNAseq data are available in the NCBI Gene Expression Omnibus, accession number GSE216420.

In Situ Hybridization and Immunohistochemistry. The RNAscope platform (ACDBio) was used for in situ hybridization, according to the manufacturer's protocol and as previously described (81). All immunohistochemistry experiments were carried out according to the same general protocol, with minor modifications for some antibodies (*SI Appendix*, Table S4) according to Meinsohn et al (14). To confirm specificity of binding, a secondary antibody only control was run with each experiment (*SI Appendix*, Fig. S18). Additional detail may be found in *SI Appendix, Methods*.

Statistical Analysis. Data were analyzed by the *t* test or ANOVA, as appropriate. A Welch's correction was used in cases of unequal variances, and outliers were identified using a Grubbs outlier test and removed. Ovarian culture data were analyzed by a paired *t* test, with mouse as pairing factor. $P < 0.05$ was considered statistically significant in all cases. Graphpad prism was used for graphing and statistical analysis. For mRNAseq data, data were analyzed in DEseq2 as described above, and transcripts were considered statistically different if Padj < 0.05, with an additional requirement for Log2fc > |1| for inclusion in pathway analyses.

Data, Materials, and Software Availability. RNAseq data have been deposited in NCBI Gene Expression Omnibus (GSE216420) (82).

ACKNOWLEDGMENTS. We are grateful to Marilène Paquette at the Plateforme d'histologie et de microscopie électronique at Université de Sherbrooke and Elvy Lapointe at the Plateforme Rnomique at Universite de Sherbrooke for technical assistance with histology and RNA sequencing respectively. Vickie Roussel, Fanny Morin, Melissa Graine, Joëlle Vincent, Cynthia Tessier, and Patrick Raymond provided valuable technical assistance.

Author affiliations: [a]Centre de recherche en reproduction et fertilité, Faculté de médecine vétérinaire, Université de Montréal, St-Hyacinthe, QC J2S 2M2, Canada; [b]Pediatric Surgical Research Laboratories, Massachusetts General Hospital, Boston, MA 02114; [c]Department of Surgery, Harvard Medical School, Boston, MA 02115; and [d]Département de biologie, Université de Sherbrooke, Sherbrooke, QC J1K 0A5, Canada

1. M. A. Damario, General aspects of fertility and infertility. *Methods Mol. Biol.* **1154**, 3–23 (2014).
2. M. Vander Borght, C. Wyns, Fertility and infertility: Definition and epidemiology. *Clin. Biochem.* **62**, 2–10 (2018).
3. R. Wang *et al.*, Treatment strategies for women with WHO group II anovulation: Systematic review and network meta-analysis. *BMJ* **356**, j138 (2017).
4. J. M. O'Connell, M. E. Pepling, Primordial follicle formation - some assembly required. *Curr. Opin. Endocr. Metab. Res.* **18**, 118–127 (2021).
5. R. Lew, Natural history of ovarian function including assessment of ovarian reserve and premature ovarian failure. *Best Pract. Res. Clin. Obstet. Gynaecol.* **55**, 2–13 (2019).
6. S. J. Chon, Z. Umair, M. S. Yoon, Premature ovarian insufficiency: Past, present, and future. *Front. Cell Dev. Biol.* **9**, 672890 (2021).
7. M. E. Pepling, A. C. Spradling, Mouse ovarian germ cell cysts undergo programmed breakdown to form primordial follicles. *Dev. Biol.* **234**, 339–351 (2001).
8. M. E. Pepling *et al.*, Differences in oocyte development and estradiol sensitivity among mouse strains. *Reproduction* **139**, 349–357 (2010).
9. M. C. Meinsohn, O. E. Smith, K. Bertolin, B. D. Murphy, The orphan nuclear receptors steroidogenic factor-1 and liver receptor homolog-1: Structure, regulation, and essential roles in mammalian reproduction. *Physiol. Rev.* **99**, 1249–1279 (2019).
10. C. H. K. Hughes, B. D. Murphy, Nuclear receptors: Key regulators of somatic cell functions in the ovulatory process. *Mol. Aspects. Med.* **78**, 100937 (2021).
11. S. Domenice *et al.*, Wide spectrum of NR5A1-related phenotypes in 46, XY and 46, XX individuals. *Birth Defects Res. C Embryo Today* **108**, 309–320 (2016).
12. A. Bashamboo, K. McElreavey, NR5A1/SF-1 and development and function of the ovary. *Ann. Endocrinol. (Paris)* **71**, 177–182 (2010).
13. P. Philibert *et al.*, NR5A1 (SF-1) gene variants in a group of 26 young women with XX primary ovarian insufficiency. *Fertil. Steril.* **99**, 484–489 (2013).
14. M. C. Meinsohn *et al.*, A role for orphan nuclear receptor liver receptor homolog-1 (LRH-1, NR5A2) in primordial follicle activation. *Sci. Rep.* **11**, 1079 (2021).
15. R. Duggavathi *et al.*, Liver receptor homolog 1 is essential for ovulation. *Genes. Dev.* **22**, 1871–1876 (2008).
16. K. Bertolin, J. Gossen, K. Schoonjans, B. D. Murphy, The orphan nuclear receptor Nr5a2 is essential for luteinization in the female mouse ovary. *Endocrinology* **155**, 1931–1943 (2014).
17. E. Rotgers, A. Jorgensen, H. H. Yao, At the crossroads of fate-somatic cell lineage specification in the fetal gonad. *Endocr. Rev.* **39**, 739–759 (2018).
18. X. Luo, Y. Ikeda, K. L. Parker, A cell-specific nuclear receptor is essential for adrenal and gonadal development and sexual differentiation. *Cell* **77**, 481–490 (1994).
19. Y. Ikeda, W. H. Shen, H. A. Ingraham, K. L. Parker, Developmental expression of mouse steroidogenic factor-1, an essential regulator of the steroid hydroxylases. *Mol. Endocrinol.* **8**, 654–662 (1994).
20. Y. Ikeda *et al.*, Comparative localization of Dax-1 and Ad4BP/SF-1 during development of the hypothalamic-pituitary-gonadal axis suggests their closely related and distinct functions. *Dev. Dyn.* **220**, 363–376 (2001).
21. S. P. Jamin, N. A. Arango, Y. Mishina, M. C. Hanks, R. R. Behringer, Requirement of Bmpr1a for mullerian duct regression during male sexual development. *Nat. Genet.* **32**, 408–410 (2002).
22. P. Jeyasuria *et al.*, Cell-specific knockout of steroidogenic factor 1 reveals its essential roles in gonadal function. *Mol. Endocrinol.* **18**, 1610–1619 (2004).
23. C. Pelusi, Y. Ikeda, M. Zubair, K. L. Parker, Impaired follicle development and infertility in female mice lacking steroidogenic factor 1 in ovarian granulosa cells. *Biol. Reprod.* **79**, 1074–1083 (2008).
24. O. E. Smith *et al.*, The role of steroidogenic factor 1 (SF-1) in somatic cell function of the testes and ovaries of mature mice. *Reproduction* **165**, 1–17 (2022). 10.1530/REP-22-0049.
25. O. E. Smith *et al.*, Steroidogenic factor 1 regulation of the hypothalamic-pituitary-ovarian axis of adult female mice. *Endocrinology* **163**, bqac028 (2022).
26. M. Cardoso-Moreira *et al.*, Gene expression across mammalian organ development. *Nature* **571**, 505–509 (2019).
27. M. J. Dollinger, W. R. Holloway Jr., V. H. Denenberg, Parturition in the rat (Rattus norvegicus): Normative aspects and the temporal patterning of behaviours. *Behav. Processes* **5**, 21–37 (1980).
28. K. J. Grive, R. N. Freiman, The developmental origins of the mammalian ovarian reserve. *Development* **142**, 2554–2563 (2015).
29. P. Kezele, M. K. Skinner, Regulation of ovarian primordial follicle assembly and development by estrogen and progesterone: Endocrine model of follicle assembly. *Endocrinology* **144**, 3329–3337 (2003).
30. P. Sengupta, The laboratory rat: Relating its age with human's. *Int. J. Prev. Med.* **4**, 624–630 (2013).
31. M. J. Stonerook, J. D. Harder, Sexual maturation in female gray short-tailed opossums, monodelphis domestica, is dependent upon male stimuli. *Biol. Reprod.* **46**, 290–294 (1992).
32. P. Maitland, S. L. Ullmann, Gonadal development in the opossum, monodelphis domestica: The rete ovarii does not contribute to the steroidogenic tissues. *J. Anat.* **183**, 43–56 (1993).
33. A. L. Johnson, The avian ovary and follicle development: Some comparative and practical insights. *Turkish J. Vet. Anim. Sci.* **38**, 660–669 (2014).
34. L. A. Kamwanja, E. R. Hauser, The influence of photoperiod on the onset of puberty in the female rabbit. *J. Anim. Sci.* **56**, 1370–1375 (1983).
35. K. J. Hutt, E. A. McLaughlin, M. K. Holland, Primordial follicle activation and follicular development in the juvenile rabbit ovary. *Cell Tissue Res.* **326**, 809–822 (2006).

36. R. Teplitz, S. Ohno, Postnatal induction of ovogenesis in the rabbit (Oryctolagus cuniculus). *Exp. Cell Res.* **31**, 183–189 (1963).
37. I. Letunic, P. Bork, Interactive tree of life (iTOL) v5: An online tool for phylogenetic tree display and annotation. *Nucleic Acids Res.* **49**, W293–W296 (2021).
38. M. C. Shih, Y. N. Chiu, M. C. Hu, I. C. Guo, B. C. Chung, Regulation of steroid production: Analysis of Cyp11a1 promoter. *Mol. Cell Endocrinol.* **336**, 80–84 (2011).
39. K. W. Kim *et al.*, CNS-specific ablation of steroidogenic factor 1 results in impaired female reproductive function. *Mol. Endocrinol.* **24**, 1240–1250 (2010).
40. L. Zhao *et al.*, Steroidogenic factor 1 (SF1) is essential for pituitary gonadotrope function. *Development* **128**, 147–154 (2001).
41. A. Fu *et al.*, IRX3 and IRX5 collaborate during ovary development and follicle formation to establish responsive granulosa cells in the adult mousedagger. *Biol. Reprod.* **103**, 620–629 (2020).
42. A. Fu *et al.*, Dynamic expression patterns of Irx3 and Irx5 during germline nest breakdown and primordial follicle formation promote follicle survival in mouse ovaries. *PLoS Genet.* **14**, e1007488 (2018).
43. J. Xu, T. Gridley, Notch2 is required in somatic cells for breakdown of ovarian germ-cell nests and formation of primordial follicles. *BMC Biol.* **11**, 13 (2013).
44. S. Malki, G. W. van der Heijden, K. A. O'Donnell, S. L. Martin, A. Bortvin, A role for retrotransposon LINE-1 in fetal oocyte attrition in mice. *Dev. Cell* **29**, 521–533 (2014).
45. A. Martinez-Marchal *et al.*, The DNA damage response is required for oocyte cyst breakdown and follicle formation in mice. *PLoS Genet.* **16**, e1009067 (2020).
46. M. E. Tharp, S. Malki, A. Bortvin, Maximizing the ovarian reserve in mice by evading LINE-1 genotoxicity. *Nat. Commun.* **11**, 330 (2020).
47. J. Wen *et al.*, GSK-3beta protects fetal oocytes from premature death via modulating TAp63 expression in mice. *BMC Biol.* **17**, 23 (2019).
48. M. He *et al.*, LSD1 contributes to programmed oocyte death by regulating the transcription of autophagy adaptor SQSTM1/p62. *Aging Cell* **19**, e13102 (2020).
49. T. R. Gawriluk *et al.*, Autophagy is a cell survival program for female germ cells in the murine ovary. *Reproduction* **141**, 759–765 (2011).
50. R. L. Jones, M. E. Pepling, KIT signaling regulates primordial follicle formation in the neonatal mouse ovary. *Dev. Biol.* **382**, 186–197 (2013).
51. E. Rotgers *et al.*, Constitutive expression of steroidogenic factor-1 (NR5A1) disrupts ovarian functions, fertility, and metabolic homeostasis in female mice. *FASEB J.* **35**, e21770 (2021).
52. M. E. Pepling, A. C. Spradling, Female mouse germ cells form synchronously dividing cysts. *Development* **125**, 3323–3328 (1998).
53. K. Reynaud, M. A. Driancourt, Oocyte attrition. *Mol. Cell Endocrinol.* **163**, 101–108 (2000).
54. M. E. Pepling, Follicular assembly: Mechanisms of action. *Reproduction* **143**, 139–149 (2012).
55. K. L. Hahn, J. Johnson, B. J. Beres, S. Howard, J. Wilson-Rawls, Lunatic fringe null female mice are infertile due to defects in meiotic maturation. *Development* **132**, 817–828 (2005).
56. R. Nomura *et al.*, Nr5a1 suppression during the murine fetal period optimizes ovarian development by fine-tuning notch signaling. *J. Cell Sci.* **132**, jcs223768 (2019).
57. S. Paget *et al.*, HIC1 (hypermethylated in cancer 1) SUMOylation is dispensable for DNA repair but is essential for the apoptotic DNA damage response (DDR) to irreparable DNA double-strand breaks (DSBs). *Oncotarget* **8**, 2916–2935 (2017).
58. J. B. Kerr *et al.*, DNA damage-induced primordial follicle oocyte apoptosis and loss of fertility require TAp63-mediated induction of puma and noxa. *Mol. Cell* **48**, 343–352 (2012).
59. M. Khot *et al.*, Twist1 induces chromosomal instability (CIN) in colorectal cancer cells. *Hum. Mol. Genet.* **29**, 1673–1688 (2020).
60. H. Jokela *et al.*, Fetal-derived macrophages persist and sequentially maturate in ovaries after birth in mice. *Eur. J. Immunol.* **50**, 1500–1514 (2020).
61. U. Repnik, V. Stoka, V. Turk, B. Turk, Lysosomes and lysosomal cathepsins in cell death. *Biochim. Biophys. Acta* **1824**, 22–33 (2012).
62. B. Kim, Y. Kim, P. S. Cooke, U. Ruther, J. S. Jorgensen, The fused toes locus is essential for somatic-germ cell interactions that foster germ cell maturation in developing gonads in mice. *Biol. Reprod.* **84**, 1024–1032 (2011).
63. V. H. Lee, J. H. Britt, B. S. Dunbar, Localization of laminin proteins during early follicular development in pig and rabbit ovaries. *J. Reprod. Fertil.* **108**, 115–122 (1996).
64. P. D. Lampe *et al.*, Cellular interaction of integrin alpha3beta1 with laminin 5 promotes gap junctional communication. *J. Cell Biol.* **143**, 1735–1747 (1998).
65. J. J. N. Burton, A. J. Luke, M. E. Pepling, Regulation of mouse primordial follicle formation by signaling through the PI3K pathwaydagger. *Biol. Reprod.* **106**, 515–525 (2022).
66. A. N. Combes *et al.*, Gonadal defects in Cited2-mutant mice indicate a role for SF1 in both testis and ovary differentiation. *Int. J. Dev. Biol.* **54**, 683–689 (2010).
67. M. Chen *et al.*, Wt1 directs the lineage specification of sertoli and granulosa cells by repressing Sf1 expression. *Development* **144**, 44–53 (2017).
68. K. Takasawa *et al.*, FOXL2 transcriptionally represses Sf1 expression by antagonizing WT1 during ovarian development in mice. *FASEB J.* **28**, 2020–2028 (2014).
69. J. Fan, E. Campioli, C. Sottas, B. Zirkin, V. Papadopoulos, Amhr2-cre-mediated global tspo knockout. *J. Endocr. Soc.* **4**, bvaa001 (2020).
70. J. A. Hernandez Gifford, M. E. Hunzicker-Dunn, J. H. Nilson, Conditional deletion of beta-catenin mediated by Amhr2cre in mice causes female infertility. *Biol. Reprod.* **80**, 1282–1292 (2009).
71. V. Selvaraj *et al.*, Commentary: Amhr2-Cre-mediated global tspo knockout. *Front. Endocrinol. (Lausanne)* **11**, 472 (2020).
72. K. Morohashi *et al.*, Structural and functional abnormalities in the spleen of an mFtz-F1 gene-disrupted mouse. *Blood* **93**, 1586–1594 (1999).
73. L. Zhao, M. Bakke, K. L. Parker, Pituitary-specific knockout of steroidogenic factor 1. *Mol. Cell Endocrinol.* **185**, 27–32 (2001).
74. A. Coste *et al.*, LRH-1-mediated glucocorticoid synthesis in enterocytes protects against inflammatory bowel disease. *Proc. Natl. Acad. Sci. U.S.A.* **104**, 13098–13103 (2007).
75. J. A. Parrott, M. K. Skinner, Kit-ligand/stem cell factor induces primordial follicle development and initiates folliculogenesis. *Endocrinology* **140**, 4262–4271 (1999).
76. C. Zhou, W. Wang, J. Peretz, J. A. Flaws, Bisphenol A exposure inhibits germ cell nest breakdown by reducing apoptosis in cultured neonatal mouse ovaries. *Reprod. Toxicol.* **57**, 87–99 (2015).
77. P. R. Hannon, S. Niermann, J. A. Flaws, Acute exposure to Di(2-Ethylhexyl) phthalate in adulthood causes adverse reproductive outcomes later in life and accelerates reproductive aging in female mice. *Toxicol. Sci.* **150**, 97–108 (2016).
78. G. de Sena Brandine, A. D. Smith, Falco: High-speed FastQC emulation for quality control of sequencing data. *F1000Res* **8**, 1874 (2019).
79. M. Bourgey *et al.*, GenPipes: An open-source framework for distributed and scalable genomic analyses. *Gigascience* **8**, giz037 (2019).
80. M. I. Love, W. Huber, S. Anders, Moderated estimation of fold change and dispersion for RNA-seq data with DESeq2. *Genome Biol.* **15**, 550 (2014).
81. M. C. Meinsohn *et al.*, Single-cell sequencing reveals suppressive transcriptional programs regulated by MIS/AMH in neonatal ovaries. *Proc. Natl. Acad. Sci. U.S.A.* **118**, e2100920118 (2021).
82. C.H.K. Hughes *et al.*, Role of steroidogenic factor 1 in the regulation of the ovarian reserve. NCBI *GEO*. https://www.ncbi.nlm.nih.gov/geo/query/acc.cgi?acc=GSE216420. Deposited 24 October 2022.